Int J Gynecol Cancer 2004, **14,** 1097–1107

A pilot study for a screening trial of cervical fluorescence spectroscopy

A. NATH*,†, K. RIVOIRE*,‡, S. CHANG§, L. WEST¶, S. B. CANTOR**, K. BASEN-ENGQUIST††, K. ADLER-STORTHZ‡‡, D. D. COX§§, E. N. ATKINSON**, G. STAERKEL¶¶, C. MACAULAY***, R. RICHARDS-KORTUM§ & M. FOLLEN*,†††,‡‡‡

**Biomedical Engineering Center, The University of Texas M.D. Anderson Cancer Center; †Department of Bioengineering, Rice University, Houston, TX; ‡Department of Physics, Massachusetts Institute of Technology, Cambridge, MA; §Department of Biomedical Engineering, The University of Texas, Austin, TX; ¶Department of Obstetrics and Gynecology, Naval Medical Center, Portsmouth, VA; **Department of Biostatistics; †† Department of Behavioral Science, The University of Texas M.D. Anderson Cancer Center; ‡‡Department of Dentistry, The University of Texas Health Science Center; ¶¶Department of Pathology, The University of Texas M.D. Anderson Cancer Center; §§Department of Statistics, Rice University, Houston, TX; ***The Department of Optical Imaging, The British Columbia Cancer Center, Vancouver, BC; †††Department of Gynecologic Oncology, The University of Texas M.D. Anderson Cancer Center; and ‡‡‡The Department of Gynecology, Obstetrics and Reproductive Sciences, The University of Texas Health Science Center at Houston, Houston, TX*

Abstract. Nath A, Rivoire K, Chang S, West L, Cantor SB, Basen-Engquist K, Adler-Storthz K, Cox DD, Atkinson EN, Staerkel G, MaCaulay C, Richards-Kortum R, Follen M. A pilot study for a screening trial of cervical fluorescence spectroscopy. *Int J Gynecol Cancer* 2004;**14:**1097–1107

Fluorescence spectroscopy is a promising technology for detection of epithelial precancers and cancers. In preparation for a multicenter phase II screening trial, a pilot trial was conducted to test data collection and patient examination procedures, use data forms, time procedures, and identify problems with preliminary data analysis. Women 18 years of age and older underwent a questionnaire, a complete history, and a physical examination, including a pan-colposcopy of the lower genital tract. A fiber-optic probe measured fluorescence excitation–emission matrices at 1–3 cervical sites for 58 women. The data collection procedures, data forms, and procedure times worked well, although collection times for all the clinical data take an average of 28 min. The clinical team followed procedures well, and the data could be retrieved from the database at all sites. The multivariate analysis algorithm correctly identified squamous normal tissue 99% of the time and columnar normal tissue only 7%. The assessment of ploidy from monolayer samples was not accurate in this small sample. The study was successful as a pilot trial. We learned who participated, who withdrew, how often abnormalities were present, and that algorithms that have worked extremely well in previous studies do not work as well when a few study parameters are changed. The current algorithm for diagnosis identified squamous normal tissue very accurately and did less well for columnar

Address correspondence and reprint requests to: Michele Follen, MD, PhD, UT-MD Anderson Cancer Center, Box 193, 1515 Holcombe Boulevard, Houston, TX 77030-4009. Email: mfollen@mdanderson.org

normal tissue. Inflammation may be an explanation for this phenomenon. Fluorescence spectroscopy is a promising technology for the detection of epithelial precancers and cancers. The screening trial of fluorescence and reflectance spectroscopy was successful.

KEYWORDS: cervix, fluorescence spectroscopy, pilot study, probe pressure, squamous intraepithelial lesions, technology assessment.

Cervical cancer is an expensive problem in the developed world and a devastating problem in the developing world. Optical technologies, which provide a diagnosis in real time, have the potential to impact both worlds substantially. As these devices can be constructed for as little as US$4000, they would be affordable in the developing world and cost-effective in the developed world[1–3]. Novel optical approaches for diagnosis include reflectance spectroscopy[4–6], fluorescence spectroscopy[7–9], Raman spectroscopy[10], confocal imaging[11], and optical coherence tomography[12].

Of these, the most widespread clinical technique for the detection of neoplasia has been fluorescence spectroscopy, which has demonstrated a sensitivity and specificity of 86 and 74% in the diagnostic colposcopy clinic and 75 and 80%[13–16] in the screening setting. Two meta-analyses have been published examining the potential applicability of fluorescence spectroscopy for screening and diagnosis. For screening, fluorescence spectroscopy was compared to the Papanicolaou's smear using receiver operating characteristic (ROC) curve analysis in a population of women expected to have a normal Papanicolaou's smear. For diagnosis, fluorescence spectroscopy was compared to colposcopy using the ROC curve in a diagnostic population of women with abnormal Papanicolaou's smears[17,18]. As shown in Figure 1, it compares favorably to the standard of care in both cases. This suggests it should be developed further as an optical technology tool.

In preparation for a large phase II study of screening fluorescence and reflectance spectroscopy, we designed and executed a pilot screening trial to test data collection and patient examination procedures, use data forms designed for the trial, time procedures for the collection of data and examination of patients, and identify problems with preliminary data analysis. We wanted to assure the database was accessible to colleagues at all three study centers. Additionally, we tested the quality assurance procedures in place for the trials.

A multivariate statistical analysis was used to identify squamous and columnar epithelial tissues and also to detect a presence or absence of dysplasia. The primary difference between the two aforementioned types of tissue is their physical structure. Squamous epithelial tissues are flat ('squama' is Latin for fish-scale), while columnar epithelial tissues are grape-like clusters of adenomatous glands. The quantitative pathology algorithm for cytology was to be tested as well.

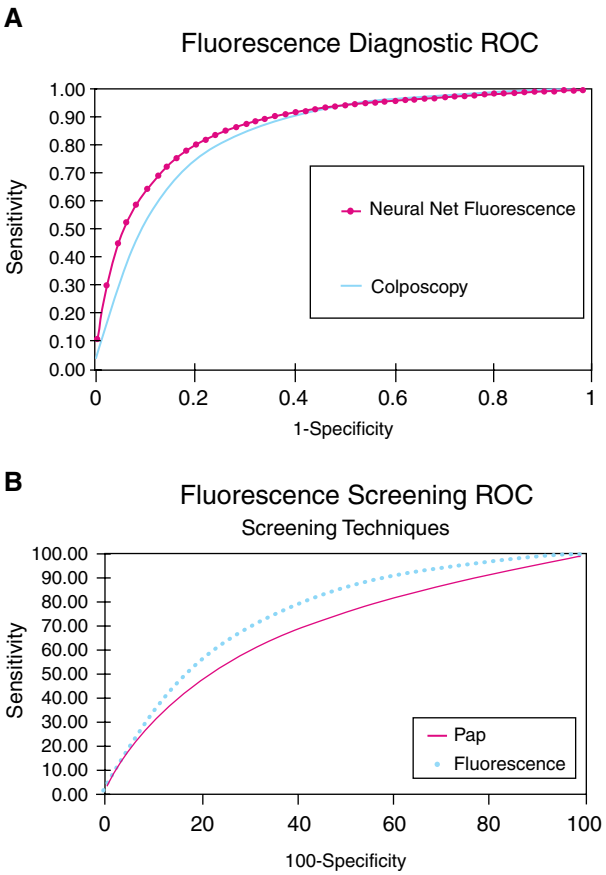

Fig. 1. A) Superimposed receiver operating characteristic (ROC) curves for fluorescence spectroscopy and colposcopy for diagnosis in a colposcopy clinic setting in which all patients referred have an abnormal Papanicolaou's smear. B) Superimposed ROC curves for fluorescence spectroscopy and the Papanicolaou's smear for diagnosis in a screening clinic setting in which all patients referred would be expected to have a normal Papanicolaou's smear.

Materials and methods

Clinical measurements

The study protocol was reviewed and approved by the Institutional Review Boards at The University of Texas M. D. Anderson Cancer Center (MDACC) and The University of Texas at Austin. Figure 2 shows a flow diagram of the study procedure. Study was conducted on site at MDACC. Eligible patients included those over the age of 18 years who were not pregnant. Driver's license information (eg, name and address) was collected as were the names of relatives so that we could contact patients in the event that their Papanicolaou's smears were abnormal. Initially, each patient underwent a urine pregnancy test, chlamydia and gonorrhea cultures, and a Papanicolaou's smear. After being explained the various details of the study and signing an informed consent, all patients underwent a demographic interview, a risk-factor questionnaire, a complete history, a physical examination, and a pan-colposcopy of the vulva, vagina, and cervix. Additionally, patients underwent Virapap testing (DiGene, Bethesda, MD) as well as human papillomavirus (HPV) DNA and mRNA sampling. This trial did not require biopsies at measurement sites.

Before use, a fiber-optic probe was disinfected with Metricide (Metrex Research Corp., Orange, CA) for 20 min. The probe was then rinsed with water and dried with sterile gauze. Prior to the placement of the probe, acetic acid was applied to the cervical epithelium. This enhanced the fluorescence and the reflectance differences between normal and dysplastic tissue.

The disinfected probe was guided into the vagina, and its tip was positioned flush with the cervical epithelium. If noticeable bleeding was observed immediately before the optical measurement, the blood was removed from the measurement site and probe tip using an alcohol swab. Fluorescence excitation–emission matrices (EEMs) were obtained from two to three colposcopically normal sites of the cervix. Measurements were taken of squamous epithelial sites, and also columnar epithelial sites, if colposcopically visible. Data collection for each EEM required approximately 2.5 min to obtain the sample. As a negative control, a background EEM was obtained with the probe immersed in a nonfluorescent bottle filled with distilled water at the beginning of each day. At the beginning of each patient's measurement, a fluorescence EEM was taken with the probe placed on the surface of a quartz cuvette containing a solution of Rhodamine 610 (Exciton, Dayton, OH) dissolved in ethylene glycol (2 mg/ml).

To correct for the nonuniform spectral response of the detection system, the spectra of two calibrated sources were measured at the beginning of the study. In the visible spectrum, a National Institute of Standards and Technology traceable calibrated tungsten ribbon filament lamp was used, while in the ultraviolet spectrum, a deuterium lamp was used (550C and 45D; Optronic Laboratories Inc., Orlando, FL). Correction factors were derived from these spectra. EEMs with dark current subtracted were then corrected for the nonuniform spectral response of the detection system. Corrections were made to variations in the intensity of the fluorescence excitation light source at different excitation wavelengths. These corrections were made with a calibrated photodiode (818-UV, Newport Research Corp., Irvine, CA) placed at the probe tip. The probe then measured intensity at each excitation wavelength.

Instrumentation

The spectroscopic system used to measure fluorescence EEMs has been described in detail previously[9], but is briefly reviewed here. The system, shown in Figure 3, measures fluorescence emission spectra at 16 excitation wavelengths, ranging from 330 to 480 nm in 10 nm increments with a spectral resolution of 5 nm. The system incorporates a fiber-optic probe, a xenon arc lamp coupled to a monochromator to provide excitation light, and a polychromator and thermoelectrically cooled charge-coupled device (CCD) camera to record fluorescence intensity as a function of emission wavelength.

Several modifications were made to the system in this study. The xenon arc lamp was replaced with a mercury lamp. Fluorescence emission as well as reflectance signals were collected by the fiber-optic probe and coupled into a scanning imaging spectrograph fitted with a high-sensitivity CCD array. The EEM collection time is optimized with the CCD-fitted spectrograph, because multiple emission intensities are read simultaneously. The excitation wavelength range was extended to a range of 290–500 nm, and emission was collected at 300–700 nm. Figure 4 shows a sample EEM recording.

Samples

The cytologic samples for clinical care were read in blinded fashion. The samples were first read by the clinical cytologist on call for the service, then by the study cytologist, then again by the cytologist on call. Discrepancies were resolved at the third reading. A companion sample was sent for image analysis. The

sample was placed in Cytyc® solution and the placed on a slide. A Feulgen–thionin stain was performed.

Image analysis

Image analysis was performed using an in-house modified version of the Cyto-Savant® automated quantitative system (Vancouver, BC, Canada). This system, pictured in Figure 5(a), includes a 12-bit double-correlated sampling MicroImager 1400 digital camera (pixels 6.8 mm^2). This software was specially designed for semiautomatic analysis of tissue sections. Feulgen–thionin stained nuclei were measured with a monochromatic light at a wavelength of 600 nm, using a 20X*0.75 NA Plan Apo objective lens. Figure 5(b) shows samples stained for analysis, and Figure 5(c) displays a software interface used for image analysis.

Quality control

The cytotechnologist manually reviewed each object in an image gallery of all the selected cells and removed any object which did not fulfill the minimum requirements (bad mask, out of focus, pale nucleus, pycnotic nucleus, etc.).

Feature calculation

Nuclear features were extracted from the digitized nuclear images of each selected cell. Table 1 summarizes the list of the features organized into different categories; approximately 120 features are calculated[20–23]. Morphologic features describe the nuclear size, shape, and boundary irregularities. The eight photometric features estimate the absolute intensity, optical density levels of the nucleus, and the intensity distribution characteristics. DNA amount is the raw measurement of the integrated optical density (IOD) from which all the photometric features are derived. The IOD norm is the mean value of the DNA amount of the reference population. The DNA index is the normalized measure of the IOD of the object, ie, DNA amount divided by IOD norm.

Texture features

Discrete texture features are based on thresholded segmentation of the object into regions of low, medium, and high optical density. The thresholds are scaled to the sample staining intensity as represented by the IOD norm value determined from the reference population. Details of algorithms are described elsewhere[18–21]. Discrete texture features are by definition dependent on the normalization. Markovian texture features characterize gray-level correlation between adjacent pixels in the image. Non-Markovian texture features describe the texture in terms of local maxima and minima of gray-level differences in the object. Fractal texture features describe the texture using local differences integrated over the object at multiple resolutions. Run-length texture features describe chromatin distribution in terms of the length of consecutive pixels with the same compressed gray-level value along different orientations (0°, 45°, 90°, and 135°). To make the run-length features rotationally invariant, we used only the mean and standard deviation over the four directions for each run-length feature.

Table 1. Patients' demographics

Patients	
Included	54
Excluded	4
Examinations	
Physical	58
Pelvic	56
Pap	56
Age	
Range	21–78
Mean	43.7
Median	43
Race	
African-American or African	7/58 (12%)
Asian	6/58 (10%)
Hispanic	16/58 (28%)
White	29/58 (50%)
Education	
Some secondary	4/58 (7%)
High school or GED	4/58 (7%)
Some college	22/58 (38%)
Bachelor's	15/58 (26%)
Some graduate school	2/58 (3%)
Advanced degree	11/58 (19%)
Gravidity (frequency)	
Range	0–8
Mean	2
Smoking	
Yes	16/58 (28%)
No	42/58 (72%)
Menopausal status	
Premenopausal	35/58 (60%)
Perimenopausal	8/58 (14%)
Postmenopausal	15/58 (26%)
Hormones by menopausal status	
Premenopausal	35
OCP use	4/35 (11%)
Perimenopausal	8
HRT use	1/8 (12%)
Postmenopausal	15
HRT use	5/15 (33%)

HRT, hormone replacement therapy; OCP, oral contraceptive.

HPV testing

Cervical samples were tested for HPV using polymerase chair reaction (PCR) and the Hybrid Capture II method (Digene Corporation, Beltsville, MD). A nucleic acid hybridization microplate assay with signal amplification for the chemiluminescent detection of HPV DNA and the Hybrid Capture II test identifies both low-risk HPV types (6, 11, 42, 43, 44) and high-risk HPV types (16, 18, 31, 33, 35, 39, 45, 51, 52, 56, 58, 59, 68).

After collection by cytobrush, cervical specimens were placed in microcentrifuge tubes containing phosphate-buffered saline with 0.05% sodium azide and frozen at −20 °C. DNA was extracted using the QI Aamp DNA Mini Kit (Qiagen, Valencia, CA) after thawing. Brushes stayed in the tubes through the cell lysis step. In the final suspension, the volume of DNA was 110 µl. PCR was performed with primers meant to amplify glycerol-3-phosphate dehydrogenase gene, the housekeeping gene, to ensure the integrity of the DNA. PCR products were resolved using electrophoresis in a 1.5% agarose gel and stained with ethidium bromide. Successful amplification was indicated by the detection of a 213-bp product. Following the methods of Manos *et al*.[7], we then analyzed samples for HPV DNA using MY9 and MY11, consensus HPV primers that amplify a 450-bp region of the L1 open-reading frame of at least 28 different HPV types. PCR products were resolved, transferred to nylon membranes (Bio-Rad Laboratories, Hercules, CA), and hybridized to ^{32}P-labeled consensus HPV 16 and HPV 18 probes. The membranes, a separate one for each probe, were inserted in X-ray cassettes overnight at −80 °C before autoradiographing. DNA extracted from HPV 18-positive HeLa cells, HPV 16-positive Caski cells, and a negative control without DNA were used as controls in the PCR and subsequent hybridization.

Statistical analyses

Data were taken from the database. Missing data were recovered from study charts. Simple descriptive statistics were performed using Microsoft Excel on the dichotomous variables.

Statistical analyses of the quantitative cytohistopathologic data

Linear discriminant analysis was used to assess the diagnostic information in the different feature set on a cell-by-cell basis. For the cell-by-cell analysis, four diagnostic comparisons were made: normal versus diploid, normal versus cycling, normal versus tetraploid, and normal versus aneuploid. All discriminant analyses were performed using the same F-to-enter and F-to-remove value of 20 for a forward stepwise analysis. The main focus of this study is to compare the relative discriminant power of the different feature sets. We performed the analysis in this fashion rather than preselecting the number of features to be included in the discriminant function. *F*-values were chosen to avoid over-training, especially for the sample-by-sample analyses, in which the initial number of features is about the same as the number of cases. All statistical analyses were performed with the STATISTICATM package produced by StatSoft, Inc. (Tulsa, OK). Only the aneuploid cell data are presented[20–23].

Multivariate analysis algorithm of the fluorescence data

The development of the multivariate statistical algorithm can be characterized by five steps. The first involves preprocessing of the spectra to reduce interpatient and intrapatient variation of spectra from a diagnostic category. Three methods of preprocessing were invoked on the spectral data at each excitation wavelength: normalization, mean-scaling, and a combination of normalization and mean-scaling. The second step involves dimension reduction of the preprocessed spectra using principle component analysis. Third, diagnostically important principle components were selected using a one-sided unpaired *t*-test. The fourth step involved the development of a probability-based classification algorithm using logistic discrimination. Finally, the retrospective and prospective evaluation of the algorithm's accuracy was examined[6–8].

Results

Patients

Fifty-eight patients participated in the study from 16 March 2000 to 8 August 2002, as summarized in Table 1. The demographics of this patient group showed that we were able to recruit a diverse population. The fact that the study was conducted at one site, here at MDACC, might account for the fact that 60% of the patients were high income and 86% were highly educated. Plans are being made to expand the study to Vancouver where Native American and more Asian and Pacific Islander patients will be accrued.

We also learned many Houstonian patients were African not African-American. Many women who are Indian, from India, called themselves Black. Having as many ethnic groups participate as possible is a good part of the study. This will allow the study results to be generalized to different populations in many parts of the world.

The distribution of menopausal status is presented in Table 2. Only a small fraction of patients are taking the oral contraceptive at this time. Similarly, only a small number of women are taking hormone replacement therapy. This is very different compared to patients in our former studies, in which up to 50% of premenopausal women were taking the oral contraceptive.

Many of the patients who chose to participate in this pilot study were not currently sexually active; this may be an explanation for why some patients could not tolerate the speculum examination. Similar to our former studies, 31% of our peri- and postmenopausal patients were taking hormone replacement therapy. As we are studying tissue estrogenization, this allows us to estimate accrual for the larger trial.

Table 2. Distribution of menopausal status

Clinical cytologic diagnosis	
Not performed	2/58
Negative for dysplasia	50/56 (89%)
Abnormal	6/56 (11%)
Cytologic acute inflammation	
Not performed	2/58
Yes	28/56 (50%)
No	28/56 (50%)
Aneuploid by DNA index	
Not performed	4/58
Yes	6/54 (11%)
No	48/54 (89%)
Hybrid Capture	
Not performed	3/55
Negative	49/55 (88%)
High risk	2/55 (4%)
Low risk	2/55 (4%)
High and low risk	2/55 (4%)
PCR DNA consensus	
Not performed	10/58
Positive	37/48 (77%)
Negative	11/48 (23%)
Colposcopic measurements	
Total number of patients	54
With three sites	8
With two sites	46
Concordance among colposcopy and fluorescence spectroscopy classification on first attempt	40/58 (69%)

Exclusions

Spectra were obtained from 54 of the 58 women. Four patients were excluded from the analysis because they were not measured. Three of the four excluded patients were unable to tolerate the speculum examination and asked to be removed from the study after participating in the questionnaire and remainder of the physical examination. The fourth patient was found to have dangerously high blood pressure, and she was sent to the emergency room for treatment of her medical condition. As expected, four of 58 (7%) of those recruited withdrew. As in many studies, up to 10% of the sample size can be expected to withdraw. This allows us to estimate what sample size is needed for the larger trial.

Trial measurements

Collection times

Figure 2 shows the flow of patients and the measurements taken during the study and the data collection procedures. The timing of the procedures is being collected as part of a time–cost study. The history took an average of 12 min (95% confidence interval CI of 6–20). The physical examination took an average of 6 min (95% CI, 4–12). Collection of fluorescence and reflectance measurements averaged 6 min (95% CI, 4–10). The colposcopy and colposcopically directed biopsy took an average of 4 min (95% CI, 2–10). All these data were collected from the 58 patients, except for the patient with hypertension noted below. Study procedures took a mean of 28 min with a minimum of 16 min and a maximum of 52 min.

Cultures, cytologies, and HPV testing

All of the patients underwent testing of their urine for pregnancy, and all test results were negative. All gonorrhea and chlamydia cultures were negative as well. While the HPV PCR demonstrated that 77% were positive, hybrid capture showed that six of 55 (11%) were positive. These findings are consistent with those in the literature. This showed us that we could not use the PCR results for clinical testing, but only for research.

Table 2 summarizes the cytologic diagnoses, presence of inflammation, quantitative cytologic results, and HPV results. As expected in a screening population, six of 58 (10%) of the patients had an abnormality. On first review, two of these six had abnormal cells consistent with HPV, while the other four patients had squamous atypias with or without cells of dysplasia. On the third blinded review, only two of these

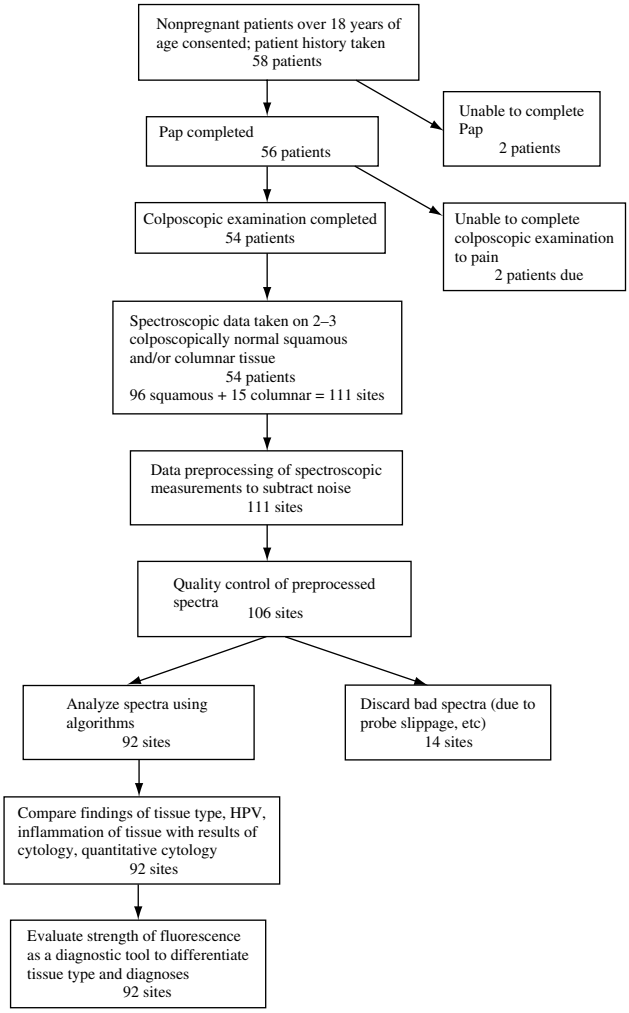

Fig. 2. Flowchart describing the conduct of the pilot screening trial and flow of data.

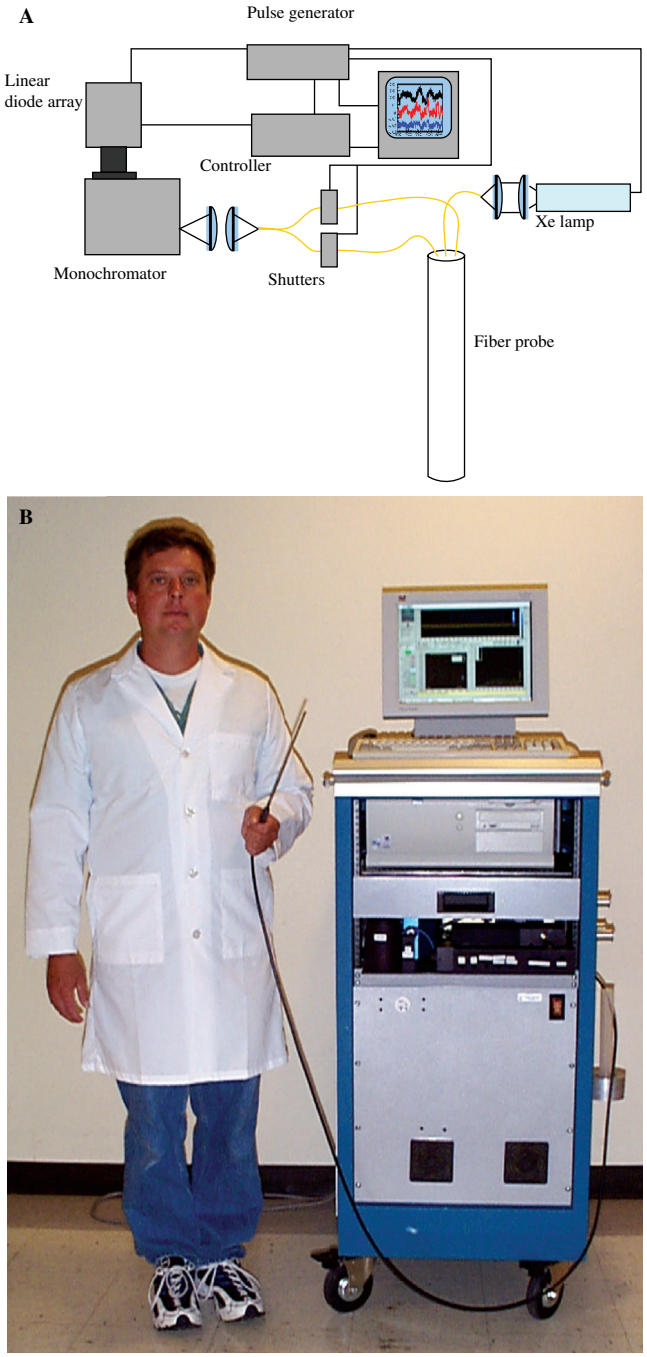

Fig. 3. A) This is a system block diagram or cartoon showing an excitation light source assembly, a fiber-optic delivery system and collection probe, and a polychromator assembly; B) A photograph of the actual device built by our laboratory and being used in the clinic for the pilot trial.

cytologies were persistently abnormal. This is very important information, as it tells us that the first clinical reading, performed by the clinical hospital group, may be over-called compared to the final reading.

By cytology, 28 patients had acute inflammation. As the gonorrhea and chlamydia cultures are all negative, we have no explanation for this finding. This is of interest, however, and may be another of the many reasons for the high costs of evaluating the abnormal Papanicolaou's smear. We will be exploring inflammation in the larger trial.

Spectroscopy results

Table 2 summarizes the colposcopic impression of the sites that were measured in each patient. As can be observed, two to three sites were measured in each patient who participated. The algorithm described by Ramanujam *et al*. was used to analyze the data obtained from the measurements, and the diagnostic output is listed in Table 2, as agreement. One of the gold standards for the analysis was the colposcopic impression, because biopsies were not performed. The ideal study design would include biopsies because the only way to know what is in the tissue

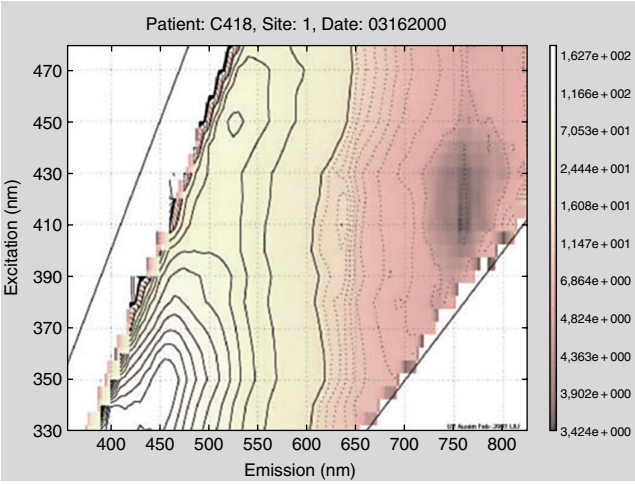

Fig. 4. This is an example of a fluorescence excitation/emission matrix taken from the cervix.

is with a biopsy. The larger trial, for which we are preparing, is designed to use biopsies as the endpoint.

The algorithm was analyzed by two of the authors after the data had been quality assured in the usual manner by three other authors. This demonstrates that data in the study is accessible to all investigators at all the sites and is analyzed by all groups participating in the trial. In summary, squamous normal sites were correctly diagnosed in 87 of 88 (99%) measurements, while columnar normal sites were only correctly identified one of 14 (7%) of the time by the algorithm.

A second analysis of the algorithm was performed using the endpoint of cytologic diagnosis. Only six Papanicolaou's smears were abnormal. When the six smears were reviewed three times, four smears were reread as normal; thus, only two were in the final pool as abnormal. Thus, we learned that on review, fewer abnormalities were likely to be present. The algorithm was unable to distinguish these two abnormalities. As they were both read only as atypias, this would require that the algorithm be capable of making very subtle diagnosis. Distinguishing high-grade from low-grade lesions is probably a more realistic goal for a device such as this one.

Obviously, large sample sizes are necessary for such studies, to study variables such as those in the fluorescence spectroscopy and those in the quantitative pathology. The threshold for these abnormalities is very low; however, we would not expect to have the algorithm threshold so low as to diagnose two atypias.

A third analysis was performed using HPV positive by Hybrid Capture. There were six cases that were positive by Hybrid Capture. The algorithm similarly was not able to recognize these six cases, but the sample size was too small for the large data set.

Quantitative pathology

The quantitative pathology findings demonstrated that six of 54 (11%) of the patients had aneuploid scores. The aneuploid cell analysis did not predict which cytologies were abnormal. As a matter of quality assurance, the pathology core did notify the clinical arm of the study of the scores. The slides were reviewed a second and third time. Four of the six patients were HPV positive by PCR, and only two by Hybrid Capture. These slides did not show inflammation. The algorithm used for the Cyto-Savant® is highly trained but has been trained on air-dried specimens. These specimens are coming from ThinPrep® specimens in Cytyc® monolayer solution, and the algorithm may need to be adjusted for these findings. This is an evolving science, and this pilot study has helped us prepare for this algorithmic issue as well.

Discussion

Optical technologies have the potential to revolutionize the practice of medicine. Real-time diagnosis, once validated, could cut down many patient visits in both developing and developed worlds. In the developing countries, this would allow less infrastructure in cytology and pathology to be developed, and hence, health dollars could be spent on rapidly diagnosing and then treating patients. In developed countries, the impact of real-time diagnosis is fewer biopsies and fewer patient visits, thus lower health care costs.

Before commencing multicenter clinical trials, studies benefit greatly from trial runs of essential data collection and patient examination procedures. The design of this trial was that the colposcopic diagnosis was used as the gold standard for the algorithm in the trial. A trial design with a biopsy at each site is clearly the ideal design, and a larger trial is presently being designed in that way. The opportunity of this study provided time to clarify the use of data forms for patient enrollment, data collection during measurements, and follow-up. We also discovered that many patients were motivated to participate because they lacked insurance, and if they did have an abnormality, a solution for their follow-up care would need to be found. The trial additionally gave us the projected time requirement for data collection procedures, including times for interviewing, physical examination, measurement, data entry, waiting for Papanicolaou's

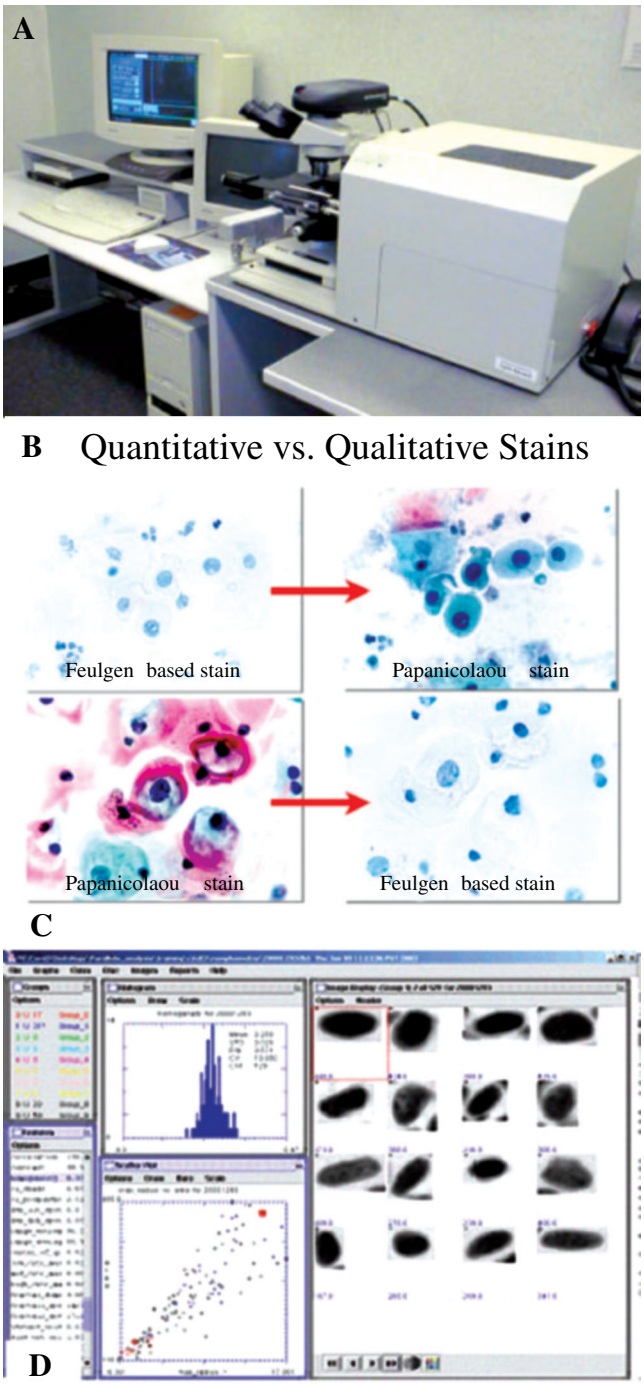

Fig. 5. A) The image cytometer, the Cyto-Savant®, used to note the quantitative cytologic measurements. B) A representation of how the Feulgen–thionin and Papanicolaou-stained Papanicolaou's smears are used for quantitative analysis. C) The steps of the semiautomated analysis of cervical lesions with A, defined area for the region of interest being measured; B, automatic locations of the positions of the nuclei; C, automatic segmentation of the nuclei in the intermediate layers of the epithelium; D, snapshot of the interface of our software used for postanalysis of the morphometric analyses (quality control).

results, and data analysis. As investigators in this trial are at three sites, this trial gave us the opportunity to test the accessibility of the database. We learned who participated, who withdrew, how often abnormalities were present, and that algorithms that have worked extremely well in previous studies do not work as well when a few study parameters are changed.

The reason for the algorithm not recognizing the columnar epithelium as easily as the squamous epithelium is unknown. We postulate this is due to inflammation, HPV, tissue structure, or an artifact of measurement with the current instrument. Columnar tissue and inflamed tissue have peak fluorescence emission at a level similar to that of squamous intraepithelial lesion (SIL)[17].

At 337-nm excitation, the spectra of columnar tissue and tissue with inflammation are indistinguishable from SIL[14]. The use of 380-nm excitation wavelength provides better differentiation of columnar and inflamed tissues from SIL ($77 \pm 1\%$ sensitivity and $72 \pm 9\%$ specificity)[14,17]. A composite algorithm utilizing measurements from 337, 380, and 460 nm was further found to improve diagnostic capabilities for differentiating columnar tissue from SIL[15]. In spite of these algorithmic improvements, however, further information is needed regarding the spectra of columnar and inflamed tissues.

An explanation for the poor detection of columnar tissue could be that the tissue was infected with HPV, which has been strongly linked with cervical cancer[23]. HPV is known to take on a latent form in some women, making it difficult to detect[24]. Results of new HPV testing can be correlated with changes in the emission spectrum of a patient, not only due to HPV infection, but also due to an inactive HPV virus. Several methods of HPV testing currently exist. The Hybrid Capture assay, a relatively easy method, has been found to have a sensitivity of 71.2% and a specificity of 92.6%[25]. The DNA PCR-based method has been found to detect 92.1% positive results; it is the more sensitive test, but it is also more difficult to perform[26]. A third method, RNA PCR, is also employed in HPV testing. An HPV-characteristic spectral signature might be present. We are currently studying the presence of the virus at several levels.

It might also be likely that the unwieldy, grape-like structure of columnar tissues (unlike the flatness of squamous cells) causes difficulty in obtaining an accurate reading from the probe. Another problem is that columnar epithelium is not visible in all patients. As the larger study will have a sample size of 1000

patients, there should be sufficient columnar measurements to help with this algorithmic issue.

In addition to this, previous studies used to create the algorithm were conducted with only one (337 nm) or three (337, 380, and 460 nm) excitation wavelengths[14,15,17]. Perhaps spectra taken at additional excitation wavelengths could reveal further differences between inflamed and columnar tissue as compared with SIL, just as using three excitation wavelengths was shown to have greater diagnostic capabilities than using one excitation wavelength[14,15]. The larger phase II screening trial, which will be making measurements at excitation wavelengths from 290 to 380 with biopsies, should clarify the signature of inflammation.

This small study is a first step toward clarifying study procedures, verifying study tools, and training the clinical and research team in procedures. Many of the results are illuminating and present valuable information; however, difficulties encountered show that further studies and improvements are necessary.

Acknowledgments

Support is gratefully acknowledged from NCI, Program Project Grant PO1 CA 82710-04. We thank providers Judy Sandella, Alma Sbach, Karen Rabel, Sung Chang, Karen Basen-Engquist, and E. Neely Atkinson.

References

1 Bigio IJ, Loree TR, Mourant J. Spectroscopic diagnosis of bladder cancer with elastic light scattering. *Lasers Surg Med* 1995;**16:**350–7.
2 Alfano RR, Tang GC, Pradham A, Lam W, Choy DSJ, Opher E. Fluorescence spectra from cancerous and normal human breast and lung tissues. *IEEE J Quant Electron* 1987;**23:**1806–11.
3 Georgakoudi I, Jacobson BC, Muller MG, Sheets EE, Badizadegan K, Carr-Locke DL. NAD(P)H and collagen as in vivo quantitative fluorescent biomarkers of epithelial precancerous changes. *Cancer Res* 2002;**62:**682–7.
4 Ramanujam N, Mitchell MF, Mahadevan A *et al. In vivo* diagnosis of cervical intraepithelial neoplasia using 337-nm-excited laser-induced fluorescence. *Proc Natl Acad USA* 1994;**91:**10193–7.
5 Ramanujam N, Mitchell MF, Mahadevan A *et al.* Spectroscopic diagnosis of cervical intraepithelial neoplasia (CIN) *in vivo* using laser-induced fluorescence spectra at multiple excitation wavelengths. *Lasers Surg Med* 1996;**19:**63–74.
6 Ramanujam N, Mitchell MF, Mahadevan-Jansen A *et al.* Cervical precancer detection using a multivariate statistical algorithm based on laser-induced fluorescence spectra at multiple excitation wavelengths. *Photochem Photobiol* 1996;**64:**720–35.
7 Brookner C, Utzinger U, Staerkel G, Richards-Kortum R, Mitchell MF. Cervical fluorescence of normal women. *Lasers Surg Med* 1999;**24:**29–37.
8 Brookner C, Utzinger U, Follen M, Richards-Kortum R, Atkinson N. Effects of biographical variables on cervical fluorescence. *J Biomed Opt* (submitted).
9 Chang SK, Dawood MY, Staerkel G, Utzinger U, Richards-Kortum RR, Follen M. Fluorescence spectroscopy for cervical pre-cancer detection: is there variance across the menstrual cycle? *J Biomed Opt* 2002;**7:**595–602.
10 Drezek R, Brookner C, Pavlova I *et al.* Autofluorescence microscopy of fresh cervical tissue sections reveals alterations in tissue biochemistry with dysplasia. *Photochem Photobiol* 2001;**73:**636–41.
11 Shim MG, Song LM, Marcon NE, Wilson BC. *In vivo* near-infrared Raman spectroscopy: demonstration of feasibility during clinical gastrointestinal endoscopy. *Photochem Photobiol* 2000;**72:**146–50.
12 Heintzelman DL, Utzinger U, Fuchs H *et al.* Optical excitation wavelengths for in vivo detection of oral neoplasia using fluorescence spectroscopy. *Photochem Photobiol* 2000;**72:**103–13.
13 Agarwal A, Utzinger U, Brookner C, Pitris C, Mitchell MF, Richards-Kortum R. Fluorescence spectroscopy of the cervix: influence of acetic acid, cervical mucus and vaginal medications. *Lasers Surg Med* 1999;**25:**237–49.
14 Brookner CK, Follen M, Boiko I *et al.* Autofluorescence patterns in short-term cultures of normal cervical tissue. *Photochem Photobiol* 2000;**71:**730–6.
15 Devore JL. *Probability and Statistics for Engineering and the Sciences*, 5th edn. Pacific Grove, CA: Duxbury; 1999.
16 Westfall P, Young S. *Resampling Based Multiple Testing*. New York: John Wiley and Sons; 1993.
17 Mitchell MF, Cantor SB, Ramanujam N, Tortolero-Luna G, Richards-Kortum R. Fluorescence spectroscopy for diagnosis of squamous intraepithelial lesions of the cervix. *Obstet Gynecol* 1999;**93:**462–70.
18 Mitchell MF, Cantor SB, Brookner C, Utzinger U, Schottenfeld D, Richards-Kortum R. Screening for squamous intraepithelial lesions of the cervix with fluorescence spectroscopy. *Obstet Gynecol* 1999;**94:**889–96.
19 Zijlstra WG, Buursma A, Meeuswen-van der Roest WP. Absorption spectra of human fetal and adult oxyhemoglobin, deoxyhemoglobin, carboxyhemoglobin, and methehemoglobin. *Clin Chem* 1991;**37:**1633–8.
20 Drezek R, Sokolov K, Utzinger U *et al.* Understanding the contributions of NADH and collagen to cervical tissue fluorescence spectra: modeling, measurements and implications. *J Biomed Opt* 2001;**6:**385–96.
21 MacAulay C, Palcic B. An edge relocation segmentation algorithm. *Anal Quant Cytol Histol* 1990;**12:**165–71.
22 Korbelic J, Matisic JP, MacAulay C, Garner D, Palcic B. Discrimination of mildly dyskaryotic squamous cervical cells with or without koilocytosis using nuclear features measured by quantitative histology and automated quantitative cytology. 21st European Congress of Cytology. September 12–16, 1993, Vienna, Austria.
23 Manos M, Ting Y, Wright D, Lewis A, Broker T, Wolinsky S. Use of polymerase chain reaction amplification for detection of genital human papillomaviruses. *Cancer Cells* 1989;**7:**209–13.

24 Mahadevan A, Mitchell MF, Silva E, Thomsen S, Richards-Kortum R. Study of fluorescence properties of normal and neoplastic human cervical tissue. *Lasers Surg Med* 1993;**13:**647–55.
25 Richards-Kortum R, Mitchell MF, Ramanujam N, Mahadevan A, Thomsen S. *In vivo* fluorescence spectroscopy: Potential for non-invasive, automated diagnosis of cervical intraepithelial neoplasia and use of a surrogate endpoint biomarker. *J Cell Biochem* 1994;**19:**111–9.
26 Clavel C, Bory J, Rihet S *et al.* Comparative analysis of human papillomavirus detection by hybrid capture assay and routine cytologic screening to detect high-grade cervical lesions. *Int J Cancer* 1998;**75:**525.

Accepted for publication December 19, 2003